Attributing icing precipitations trend (1951-2098) in the context of climate change in Europe

Florian Raymond, Philippe Drobinski, Nicolas Roche

Climatologie 2023, 21, 1

https://doi.org/10.1051/climat/202321001

Disponible en ligne :
https://climatology.edpsciences.org

Attributing icing precipitations trend (1951-2098) in the context of climate change in Europe

Florian Raymond [1, 2], Philippe Drobinski [1], Nicolas Roche [3]

[1] LMD/IPSL, École Polytechnique, Université Paris Saclay, ENS, PSL Research University, Sorbonne Université, CNRS, Palaiseau, France

[2] Département de Géographie, Université Paris 8 Vincennes-Saint-Denis, UMR7533 Ladyss, Saint-Denis, France

[3] ENEDIS, Courbevoie, France

Abstract – Freezing rain and wet snow, both mentioned as “icing precipitation” in this study, are wintertime climatic events that can lead severe damages for environment and societies. At the European scale, only few studies focused on these climatic events, in comparison with North America. The objectives of this study is (*i*) to apprehend the actual and future spatio-temporal variability of the "high-impact Icing Precipitation favourable Days" (IPDs), and (*ii*) to explore the dominating climate variable controlling the IPD trends between the temperature (thermal conditions) and the precipitation (vulnerability conditions), because of the uncertainties of the future projections. Daily minimum, maximum near surface temperatures and accumulated precipitations from the E-OBS (historical period; 1951-2018) and from the Euro-Cordex initiative (future simulations; 2026-2098) are used to apprehend the IPDs. For the historical period, no clear trend emerges, either for the IPDs evolution and for the influential climate variable. For both the near- and long-term horizons, models simulate a decrease in the frequencies of IPDs that should affect almost all of Europe, except for the Scandinavia region. In addition, there would be a strong contribution of the temperature, climatic variable well simulated by regional models, as the most influential climatic conditions in the future variability of the IPDs.

Keywords: icing precipitation, future variability, attributing of variability, Europe.

Résumé – **Attribution de la tendance des précipitations givrantes (1951-2098) dans le contexte du changement climatique en Europe**. La pluie verglaçante et la neige collante, toutes deux mentionnées comme des « précipitations givrantes » dans cet article, sont des événements climatiques hivernaux qui peuvent entrainer de forts impacts sur les sociétés et sur l’environnement. A l'échelle européenne, peu d'études ont porté sur ces événements climatiques, en comparaison avec l'Amérique du Nord. Les objectifs de cette étude sont (*i*) d'étudier la variabilité spatio-temporelle actuelle et future des jours favorables à l’apparition d’événements de précipitations givrantes à forts impacts (« *high-impact Icing Precipitation favourable Days* » ; IPD), et (*ii*) de cerner la variable climatique de surface qui influencerait majoritairement la variabilité des IPDs, entre la température (conditions thermiques) et les précipitations (conditions de vulnérabilité), pour évaluer la robustesse des résultats en raison des incertitudes des projections futures notamment pour les précipitations. Les températures quotidiennes minimales et maximales ainsi que les cumuls quotidiens des précipitations issues de la base de données E-OBS (période historique ; 1951-2018) et de l'initiative Euro-Cordex (simulations futures ; 2026-2098) sont utilisées pour étudier les IPDs. Pour la période historique, aucune tendance claire n'émerge, que ce soit pour l'évolution des IPDs ou pour la variable climatique ayant la plus forte influence. A court et long terme, les modèles simulent une diminution des fréquences d’apparition des IPDs, qui devrait toucher la quasi-totalité de l'Europe, à l'exception de la Scandinavie. De plus, il y aurait une forte contribution de la température, variable climatique bien simulée par les modèles régionaux, comme condition climatique la plus influente dans la variabilité future des IPDs.

Mots-clés : précipitations givrantes, variabilité future, attribution, Europe.

* Corresponding author: florian.raymond02@univ-paris8.fr

The issues of the icing precipitation in Europe

Freezing rain and wet snow deposition are wintertime events causing icing formation. Stewart *et al.* (2015) define the freezing rain as "*rain that falls in liquid form but freezes upon impact to form a coating of glaze upon the ground and on exposed objects*" and the wet snow as "*snow that contains a great deal of liquid water*". The wet snow contains more water than the dry-snow, which makes it heavier than dry snow and conducive to the appearance of ice when the temperatures cool down.

Carriere *et al.* (2000) describes the thermodynamic conditions for freezing rain. It develops as falling snow encounters a layer of warm air deep enough for the snow to completely melt and become rain. As the rain continues to fall, it passes through a thin layer of cold air just above the surface and cools to a temperature below freezing. Due to supercooling phenomenon, the drops do not freeze (they form "supercooled drops"). When the supercooled drops strike the frozen ground (power lines or tree branches for example), they instantly freeze, forming a thin film of ice, hence freezing rain. Regarding wet snow, it forms when the near surface temperature is slightly higher than 0°C with precipitations whether in the form of rain, snow or mixed snow and rain (Bourguin, 2000; Forbes *et al.*, 2014).

In the following, we will refer to "icing precipitation" as the generic term referring to both freezing rain and wet snow (as defined by Bonelli *et al.*, 2011), as their conditions of occurrence are rather similar. Icing precipitation deposits can lead severe damages on trees, roads and power lines, that can result in severe loss of electrical power, transportation disruptions, school and business closings, economic loss for many sectors including agriculture and sometime in loss of life (Call, 2010; Bonelli *et al.*, 2011; Lambert *et al.*, 2011). Power lines can be affected in two ways, (*i*) potential extra weight of ice is an input for basis design and (*ii*) risk management of tree branches breaking and falling onto the lines impact pruning operations. The amount of icing precipitation controls the type of damages that it produces. For instance, precipitation amount less than 10mm is not expected to produce an important snow overload to damage a power line (Bonelli *et al.*, 2011). Ice accumulation ranging between 13 and 25mm causes serious breakage and damages healthy young trees, even though small branch failures can be caused from about 5mm (Degelia *et al.*, 2016). The US National Weather Service defines ice storm when at least about 5mm of freezing rain has fallen (USNWS, 2020). Indeed, the 14-15 February 1990, ice storm in Illinois caused more than 12 million damages with 5mm accumulated icing precipitation (Rauber *et al.*, 1994). Bendel and Paton (1981) found that the high-impact ice storm events had at least about 6mm accumulated ice. Their review of the impact of ice storms on the power industry in the USA shows that in nearly a decade between 1971 and 1978, about 20% of ice storms induced damages on the power systems exceeding 5 million USD. In Canada, the relatively rare major icing precipitation events are considered by far the costliest among all hydrometeorological disasters (Dore, 2003), often fatal events, having strong impacts on the electrical system.

Most of the studies investigate icing precipitation climatology or trend in regions severely and frequently impacted by such events, in particular North America and Eurasia (Bendel and Paton, 1981; Changnon, 2003; Cortinas *et al.*, 2004; Changnon and Bigley, 2005; Cheng *et al.*, 2007; Cheng *et al.*, 2011; Lambert and Hansen, 2011; Bulygina *et al.*, 2015; Groisman *et al.*, 2016). They show from recent past observations an increasing occurrence of icing precipitation in North America, north of the Arctic Circle, and a decreasing occurrence further South. More precisely, the current maximum icing precipitation over North-eastern America is predicted to weaken and move poleward, leading to a marked decrease in icing precipitation occurrence in Eastern USA as well as in the Atlantic provinces of Canada. North of the current maximum and across central Canada a modest increase is predicted (Cheng *et al.*, 2007; Lambert and Hansen, 2011). The icing precipitation occurrence trend is also positive in European Russia and Western Siberia (Bulygina *et al.*, 2015; Groisman *et al.*, 2016).

Compared to North America and Eurasia, Europe has conversely received much less attention in the literature while icing precipitation events

have regularly impacted European countries with significant damages and human losses. Table 1 lists some major recent events in Europe and their associated damages. Freezing rain mainly occurs between September and May in Northern Europe, and between October and April in Central and Eastern Europe (Kämäräinen *et al.*, 2017). It can extend to the Mediterranean region, if we consider wet snow (Bonelli *et al.*, 2011). Recent observations have shown an icing precipitation occurrence increase in Norway (Groisman *et al.*, 2016) and climate projections suggest a decrease in Western, Central and Southern Europe, and an increase in Northern and North-Eastern Europe (Kämäräinen *et al.*, 2018).

Table 1. List of past main freezing-rain events in Europe from the literature, including the date and impacted country, the king of events, the damages produced and the references mentioning the events. *Liste des principaux épisodes de pluie verglaçante survenus en Europe évoqués dans la littérature, comprenant la date et le pays touché, le type d'évènement, les dommages causés et les articles mentionnant les événements.*

Date	Country	Type	Damages	References
Dec. 1990	UK	Wet snow	Power outage for 30 hours to 9 days in the country	Solangi, 2018
Nov. 2005	Germany	Wet snow	82 broken transmission towers, Electrical blackout (>250 000 people impacted), Dusseldorf airport closed for several days, many roads blocked by fallen trees	Brostrom, 2007, Frick and Wernli, 2012
Mar. 2010	Spain	Wet snow	2 deaths, Power outage for 6 weeks (>450 000 people impacted), 150 000 ha of forest affected	Solangi, 2018, Llasat *et al.*, 2014
Mar. 2010	Italy	Wet snow	Power outage (>25 000 people impacted)	Bonelli *et al.*, 2011
Dec. 2010	Russia	Freezing rain	Power lines destroyed, air transport cancelled	Kämäräinen *et al.*, 2017
Feb. 2012	Italy	Wet snow	Power outage (>125 000 people impacted)	Marcacci *et al.*, 2019
Feb. 2014	Slovenia	Freezing rain	More than 200 km of power lines destroyed or inoperant, 25% of population without electricity, heating and water, 40% of Alpine forests destroyed, damages estimated at 400 million euros	Forbes *et al.*, 2014, Markosek, 2015, Kämäräinen *et al.*, 2017
Jan. 2017	Italy	Wet snow	Power outage (>300 000 people impacted)	Marcacci *et al.*, 2019
Jan. 2019	Romania	Freezing rain	2622 broken trees in Bucharest, interruption of the public transport due to power outages, 759 cars damaged	Andrei *et al.*, 2019

However, competing effects of temperature and precipitation as well as surface effects affect the evolution of the frequency, intensity and geographic distribution of impactful icing precipitation events. Also the uncertainty of climate projections differs on the projected variables, as studies suggest that precipitation projections are characterized by much higher uncertainty than temperature projections, especially at the regional scale (Giorgi, 2010). Therefore, as a follow-up of Kämäräinen *et al.* (2018), it is key to quantify the dominating factor controlling the icing precipitation trends in Europe, to attribute these trends to those of temperature and precipitation and assess their significance. Then the objectives of this study is (*i*) to apprehend the actual and future spatio-temporal variability of the impactful icing precipitation events across the whole Europe, and (*ii*) to explore the dominating climate variable

controlling the trends of these events between the temperature (thermal conditions) and the precipitation (vulnerability conditions), because of the more or less pronounced uncertainties of the future climatic projections. This study relies on the regional climate scenarios performed in the context of Euro-CORDEX downscaling experiment (Jacob *et al.*, 2014) parts of the global CORDEX program (COrdinated Downscaling EXperiment; Giorgi *et al.*, 2009).

The paper is organized as follow: Section 1 describes the datasets and methodology to identify icing precipitation occurrence. Section 2 analyses the recent past trend of icing precipitation occurrence, and assesses the performance of the regional climate simulations to reproduce the observed trend over the historical period. Section 3 quantifies the future climate trends in two scenarios and attributes the probable origin of such trends. Section 4 provides elements of discussion and Section 5 concludes the study.

1. Data and methodology

1.1. Daily precipitation and temperature data

Icing precipitation formation depends on the near surface temperature (Carriere *et al.*, 2000) while its ability to produce damages depend on the accumulated rain (Bonelli *et al.*, 2011). Recent past climatology of temperature and precipitation is analysed in the following based on surface measurements (from the E-OBS database) and reanalysis (from the ERA5 reanalysis) or historical climate simulations (from five regional climate models) performed in the context of Euro-CORDEX program. Future climate projections are analysed from simulations performed by the same five regional climate models from Euro-Cordex as the historical simulations.

1.1.1. E-OBS observations

The daily minimum, maximum temperatures and accumulated precipitation from the E-OBS gridded dataset v.22.0 are used over the 1951-2018 period (a total of 78 years) (Haylock *et al.*, 2008; Cornes *et al.*, 2018). The choice was made to cut the entire period for which we had observations data into two sub-periods of 34 years (1951-1984 and 1985-2018) to apprehend the potential changes in the climatic surface conditions between the first and the second part of the historical period. E-OBS gridded dataset, provided by the European Climate Assessment & Dataset project (ECA&D; Klok *et al.*, 2009), is available at daily time-step and a spatial resolution of 0.25° over Europe. Data observations are aggregated from 7 336, 7 263 and 14 472 weather stations over Europe, the Middle East and North Africa using an interpolation procedure combining spline interpolation and kriging. This dataset is a reference dataset for regional climate studies (Stefanon *et al.*, 2012; Raymond *et al.*, 2016; Raymond *et al.*, 2018a) and the evaluation of regional climate models (Kjellström *et al.*, 2010; Flaounas *et al.*, 2012; Kjellström *et al.*, 2013; Stefanon *et al.*, 2014; Vaittinada *et al.*, 2016; Drobinski *et al.*, 2018, Raymond *et al.*, 2018b).

Like many databases, E-OBS includes some errors and uncertainties (that can be induced by changes in station locations or interpolation uncertainties, for example). Therefore, the E-OBS dataset has been extensively evaluated in the literature (Hofstra *et al.*, 2009; Hofstra *et al.*, 2010; Kyselý and Plavcová, 2010; Flaounas *et al.*, 2012; Herrera *et al.*, 2012; Prein and Gobeit, 2017). These studies show that the E-OBS data well reproduce the spatio-temporal distribution of the precipitation and temperature series, even if extreme values tend to be underestimated, especially for precipitations in sectors with poor stations density.

1.1.2. ERA5 reanalysis

ERA5 is the fifth generation ECMWF atmospheric reanalysis of the global climate covering the period from January 1950 to present (Hersbach *et al.*, 2020). The reanalysis database provides hourly estimates of a large number of atmospheric, land and oceanic climate variables. The data cover the Earth on a 30 km grid (0.25° in latitude and longitude) and resolve the atmosphere using 137 levels from the surface up to a height of 80 km. ERA5 includes information about uncertainties for all variables at reduced spatial and temporal resolutions.

As mentioned by Vaittinada *et al.* (2021), climate simulations often need to be corrected (to get simulated series with appropriate statistical

properties) before any climate change studies. The daily temperatures and accumulated precipitation from ERA5 then are used to correct the biases in the Euro-CORDEX simulations over the 1980-2018 period (see below). Used statistical methods to reduce the bias encountered in global or regional climate model output are common to get the simulated data series closer to reference data series (such as reanalysis), in term of distribution (Vrac *et al.*, 2012; Vrac and Friederichs, 2015; Vrac *et al.*, 2016; Dosio, 2016; Vaittinada *et al.*, 2021; Xu *et al.*, 2021). ERA5 is then a data series regularly used to correct the biases in the climate simulation (Lemos *et al.*, 2020; Carvalho *et al.*, 2021; Noel *et al.*, 2021; Xu *et al.*, 2021).

As for the E-OBS data, the ERA5 reanalysis well reproduces the spatial distribution of precipitations, even if it tends to underestimate the magnitude of extreme daily precipitations in comparison to weather station data (Hu and Franzke, 2020). In other way, ERA5 reanalysis tends to underestimates temperatures in some European sub-regions (with complex topography, e.g., mainly in the Alps and the Mediterranean; Valikou *et al.*, 2022). As for E-OBS, this is not a problem for this study, which is not based on extreme values of temperature and precipitation to apprehend icing precipitation (see further).

The ERA5 is also used as an alternative source of "observation data-set" to assess the uncertainty of the Euro-CORDEX simulation datasets over the historical period 1972-2005. After 2005, the Euro-CORDEX simulations are based on greenhouse gas scenarios to simulate the climate (see below), and not anymore on the real greenhouse gas concertation previously observed in the atmosphere, because of the Global Climate Models CMIP5 temporality (which force CORDEX simulations).

1.1.3. Euro-CORDEX regional climate model simulations

Projections of icing precipitation occurrence rely on the three hourly temperatures and daily accumulated precipitation from the regional climate simulations performed in the frame of the CORDEX program in the European region (CORDEX program, Giorgi *et al.*, 2009; Euro-CORDEX initiative, Jacob *et al.*, 2014). Three hourly temperatures have been processed to obtain daily minimum and maximum temperature for the historical period (1972-2005, the near time (2026-2059) and long-time (2065-2098) horizons. Two representative concentration pathway (RCP) scenarios are used (Moss *et al.*, 2010): the RCP4.5 scenario (global radiative forcing of +4.5 W.m² by 2100, in comparison with the pre-industrial era), where the greenhouse emissions increase until 2070 and then stabilize (intermediate emission scenario); and RCP8.5 scenario (global radiative forcing of +8.5 W.m² by 2100), where emissions continue to strongly rise throughout the twenty-first century (very high emission scenario). Table 2 summarizes the five Euro-CORDEX regional climate simulations used in this study.

All regional climate simulations have been de-biased using the Cumulative Distribution Functions-transform (CDF-t; Michelangeli *et al.*, 2009) with the daily temperatures and accumulated precipitation from ERA5 as inputs of CDF-t over the 1980-2018 period (calibration period). The bias correction is evaluated over the 1972-2005 period (validation period) using E-OBS dataset, and then applied to the future climate projections.

1.2. Detection of high-impact icing precipitation favourable days

In this study, the choice is made to only used near surface temperature and precipitation with specific thresholds in order to identify days with surface conditions favourable to the occurrence of high-impact icing precipitation events. The use of the near surface temperature is explained by the fact that this climatic variable mainly explains the state in which the drop of water that falls will end up between freezing rain (weak negative near surface temperature) and wet snow (weak positive near surface temperature), as explain by the different references called in the introduction of this study. This approach, complementary to that of Kämäräinen *et al.* (2018), based on the vertical structure of freezing rain events (process-based approach), is a probabilistic approach with a method of separation between the temperature trend and the precipitation trend, on the condition there is no correlation between the meteorological parameters, which is assessed as a reasonable assumption.

Table 2. Regional climate simulations from the Euro-CORDEX initiative in the European region used in this study, which include historical simulations and future climate projections with RCP4.5 and RCP8.5 scenarios. It includes the names of the institution which produced the simulations, the names and versions of the regional climate models (RCM) and of the global climate model (GCM) used in CMIP5 that have been used to drive the RCM. It also gives the different simulations periods and the reference article for the various RCMs.

Simulations climatiques régionales de l'initiative Euro-CORDEX utilisées dans cette étude pour la région européenne, qui comprennent des simulations historiques et des projections climatiques futures avec les scénarios RCP4.5 et RCP8.5. Le tableau comprend les noms des institutions qui ont produites les simulations, les noms et les versions des modèles climatiques régionaux (MCR) et du modèle climatique global (MCG) utilisés dans CMIP5 qui ont été utilisés pour piloter le MCR. Le tableau indique également les différentes périodes de simulation disponibles et l'article de référence pour les différents MCR.

Institute	Regional model	Global model	Period covered	Reference
IPSL	WRF381P	IPSL-CM5A-MR	1951-2100	Skamarock *et al.*, 2008
KNMI	RACMO22E	ICHEC-EC-EARTH	1950-2100	Van Meijgaard *et al.*, 2008
SMHI	RCA4	MOHC-HadGEM2-ES	1970-2098	Rummukainen *et al.*, 2001
CLMcom	CCLM4	MPI-ESM-LR	1950-2100	Rockel *et al.*, 2008
DMI	HIRAM5	NCC-NorESM1-M	1951-2100	Christensen *et al.*, 2007

Additional note: IPSL = Institut Pierre-Simon Laplace; KNMI = Koninklijk Nederlands Meteorologisch Instituut; SMHI = Swedish Meteorological and Hydrological Institute; CLMcom = Climate Limited-area Modelling Community; DMI = Danish Meteorological Institute.

Various studies find freezing rain occurring for negative near surface temperatures higher than -5°C (Carrière *et al.*, 2000; Cortinas, 2000; Cortinas *et al.*, 2004) or slightly higher (between -4°C and +1°C in Bernstein, 2000). For wet snow, favourable near surface temperatures are found ranging between 0°C and +2°C (Makkonen and Wichura, 2010; Bonelli *et al.*, 2011; Solangi, 2018). Based on these studies, near surface temperatures ranging between -5°C and +2°C are considered in the following favourable conditions for icing precipitation formation.

Based on the literature reviewed in the introduction, high-impact icing precipitation events occur when daily accumulated precipitation generally exceed a threshold of 5 mm. Therefore, in this study, the risk of high-impact icing precipitation is given by the simultaneous combination of favourable *thermal condition* given by:

$$Tmin \geq -5°C \text{ and } Tmax \leq +2°C \quad (1)$$

and favourable *vulnerability condition* given by:

$$RR \geq 5 \text{ mm} \quad (2)$$

with *Tmin* the daily minimum temperature, *Tmax* the daily maximum temperature, and *RR* the daily accumulated precipitation. A day when those two conditions are simultaneously met is referred to as an "high-impact Icing Precipitation favourable Day" (IPD). In our data set, when IPD conditions are met, the grid point is tagged with a "1" and "0" otherwise (binary matrix).

Beyond the evolution's assessment of the risk of high-impact icing precipitation, we also assess the respective contributions of the thermal condition (1) and of the vulnerability condition (2) to the high-impact icing precipitation occurrence evolution. Such analysis is not only interesting in terms of attribution of the IPDs variability at stake, but also in a perspective of uncertainty assessment. Indeed, projections of temperatures which control the thermal condition are generally less uncertain than precipitation which determine the level of vulnerability and which are less reliably and accurately predicted by regional climate models especially for weak and intense precipitation (Kumar *et al.*, 2013; Sillmann *et al.*, 2013; Mehran *et al.*, 2014; Aloysius *et al.*, 2016; Bastin *et al.*, 2019).

Let us denote TCD (thermal condition day) a day when the thermal condition (1) is met and VCD (vulnerability condition day) a day when the vulnerability condition (2) is met. As for IPD, a binary matrix is used for detecting TCD or VCD days, with grid points tagged in "1" when the TCP or VCD condition is met, and "0" otherwise.

As previously said, a day when both the TCD and VCD conditions are simultaneously met is referred to as an "high-impact Icing Precipitation favourable

Day" (IPD). Therefore, the IPD probability of occurrence is P(IPD)=P(TCD⋂VCD), where P(TCD) and P(VCD) are the probabilities of occurrence of TCD and VCD, respectively. Assuming that the thermal and vulnerability conditions are independent then P(IPD)=P(TCD)P(VCD).

The evolution in the number of IPDs, relative to a 34 years reference period (1951-1984 for the historical period or 1972-2005 for the future simulations) is then:

$$\Delta P(IPD)=\Delta P(TCD)/P(TCD)+\Delta P(VCD)/P(VCD)$$

where the Δ operator is the difference between the 2 periods of 34 years (1985-2018 in comparison to 1951-1984 for the historical period; 2026-2059 or 2065-2098 in comparison to 1972-2005 for the future simulations), to include the whole natural relative variability and keep only the climatic trend.

To evaluate the robustness of the change of P(IPD), we tried to untangle the role of precipitation (vulnerability conditions) and temperature (thermal conditions) in the evolution of IPD occurrence. For future climate, the attributing of the IPDs variability (between VCD or TCD) is robust if at least 4 of the 5 models agree about the most influential climate variable. The attribution variability, for each of the studied grid-point, is defined as follows:

- if ΔP(IPD)/P(IPD)>0, the condition that dominantly controls the increase in the occurrence of IPDs is the thermal condition (TCD) if it shows a more pronounced relative increase than VCD (ΔP(TCD)/P(TCD)>ΔP(VCD)/P(VCD)), otherwise it is the vulnerability condition (VCD).
- if ΔP(IPD)/P(IPD)<0, the condition that dominantly controls the decrease in the occurrence of IPDs is the thermal condition (TCD) if it shows a more pronounced relative decrease than VCD (ΔP(TCD)/P(TCD)<ΔP(VCD)/P(VCD)), otherwise it is the vulnerability condition (VCD).

This allows to map the most influential surface climate variables on IPDs occurrence evolution.

The test of Student (T-test; 0.95 confidence level) will be used to assess the significance of the evolution of temperature and precipitation during the historical period. The Khi-2 test (0.95 confidence level) will be used to assess the significance of the evolution in the number of VCDs, TCDs and IPDs (binary matrix, change in proportions) during the different periods studied.

2. Recent past trends

2.1. E-OBS data

During the historical sub-period 1985-2018, the mean annual accumulated precipitation has evolved unevenly in Europe, in comparison to the sub-period 1951-1984 (figure 1a).

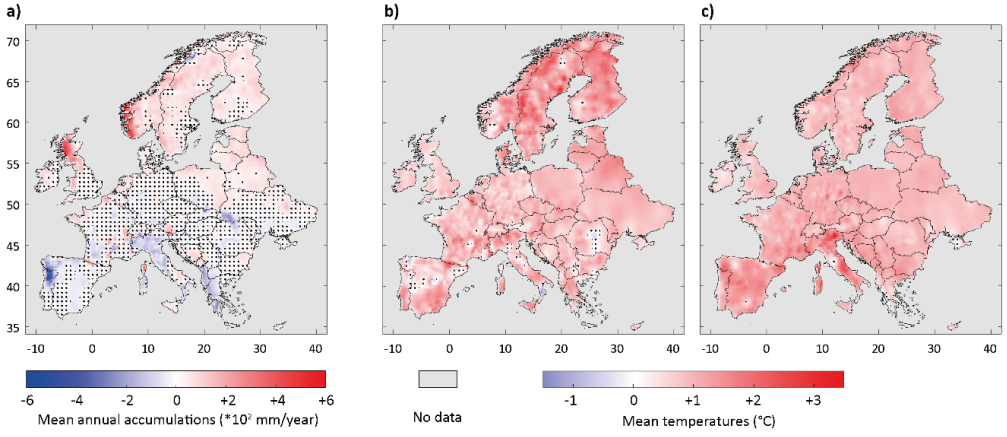

Figure 1. Evolution of a) the mean annual accumulation of precipitations (mm/year), b) the minimum and c) the maximum average temperatures (°C) in Europe from the E-OBS dataset for the period covering 1985-2018, in comparison to the period covering 1951-1984. No significant evolutions are indicated with black dotted lines, according to the T-test (at the 0.95 confidence level). In grey, sectors with no data in this study. *Évolution a) du cumul annuel moyen des précipitations (mm/an), b) des températures moyennes minimales et c) des températures moyennes maximales (°C) en Europe pour la période 1985-2018 par rapport à la période 1951-1984 (à partir de l'ensemble de données E-OBS). Les pointillés noirs indiquent qu'il n'y a pas d'évolution significative, selon le test T (au niveau de confiance de 0,95). En gris, les secteurs sans données dans cette étude.*

Northern Europe displays a significant positive trend, mainly in the UK, Scandinavia, Finland, Baltic countries. Conversely, in Southern Europe (the Mediterranean region), the trend is significantly negative. Such results are consistent with the exiting literature (Hoerling *et al.*, 2012; Van den Besselaar *et al.*, 2012; Caloiero *et al.*, 2015; Raymond *et al.*, 2016; IPCC, 2021). Unlike precipitation, temperatures, including daily minimum and maximum, have increased over whole Europe between 1951-1984 and 1985-2018 (figures 1b and 1c; Van Oldenborgh *et al.*, 2009; Gil-Alana and Sauci, 2019; IPCC, 2021). Scandinavia is the region with the most pronounced increase in minimum temperatures (more than +3°C; figure 1b), and southwestern Europe in maximum temperatures (also more than +3°C; figure 1c). As shown in Figure 1, climate change is affecting the temperatures in a more straightforward way than the precipitations over Europe, with less uncertainties. Only 56% of the studied grid points show significant evolution of the precipitations between the two historical periods (figure 1a), while between 98% and 99% show significant evolution of the temperatures (figures 1b and 1c).

Figure 2 shows the change of occurrence of the vulnerability and thermal conditions during 1985-2018, in comparison to 1951-1984. Because of the accumulated precipitation increases (*resp. decreases*) in Northern Europe (*resp. Southern Europe*), the occurrence of the vulnerability condition day (VCD) also increases (*resp. decreases*) (figure 2a).

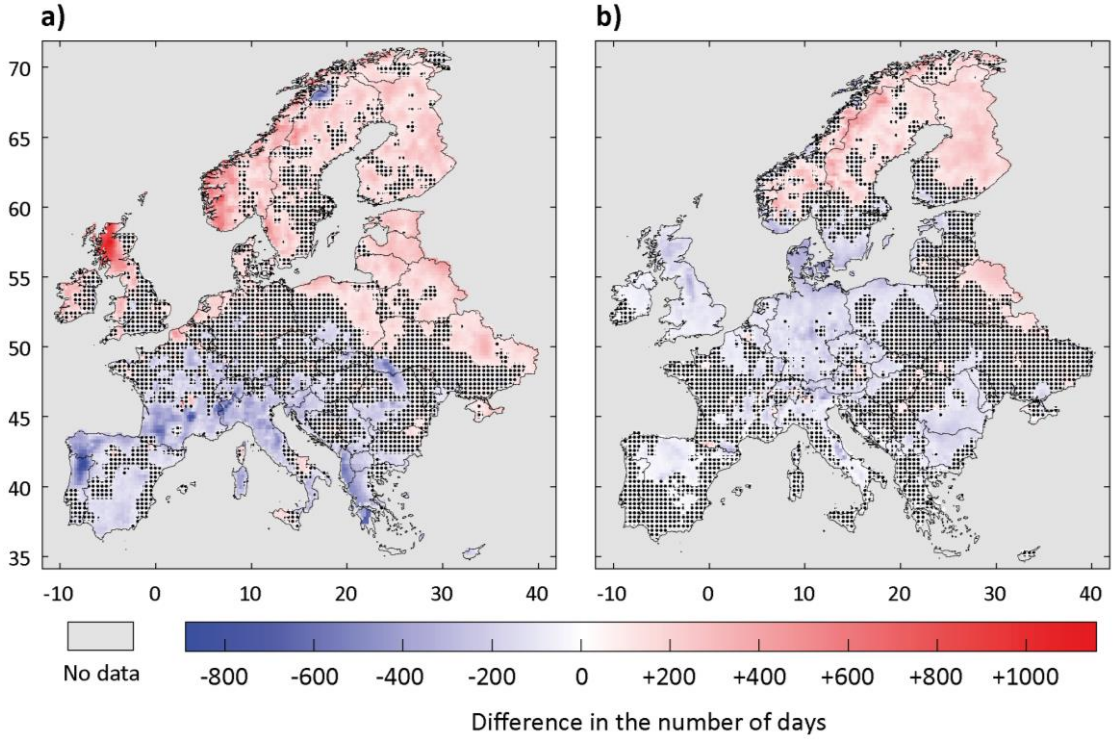

Figure 2. Spatiotemporal variability about a) the vulnerability condition day (VCD, precipitation accumulation ≥ 5 mm/day) and b) the thermal condition day (TCD, daily $T^{min} \geq -5^{\circ}C$ and $T^{max} \leq +2^{\circ}C$), favourable to the occurrence of high-impact Icing Precipitation Days (IPDs) when they occur simultaneously. Conditions are observed from the E-OBS dataset for the period covering 1985-2018, in comparison to the period covering 1951-1984. The number of days is computed through a binary matrix, with "1" when the VCD or TCD is met, and "0" when it is not the case. No significant differences are indicated with black dotted lines, according to the χ^2 test (at the 0.95 confidence level). In grey, sectors with no data in this study.

Variabilité spatio-temporelle a) du nombre de jours de condition de vulnérabilité (VCD, accumulation de précipitations ≥ 5 mm/jour) et b) du nombre de jours de condition thermique (TCD, T^{min} journalière ≥ -5◦C et $T^{max} \leq +2^{\circ}C$), favorable à l'occurrence de jours de précipitations givrantes (IPD) à fort impact lorsqu'ils se produisent simultanément. Les conditions (vulnérabilité et thermiques) sont observées à partir du jeu de données E-OBS pour la période couvrant 1985-2018 par rapport à la période couvrant 1951-1984. Le nombre de jours est calculé à l'aide d'une matrice binaire, avec "1" lorsque le VCD ou le TCD est atteint, et "0" lorsque ce n'est pas le cas. Les pointillés noirs indiquent qu'il n'y a pas de différences significatives, selon le test du χ^2 (au niveau de confiance de 0,95). En gris, les secteurs sans données dans cette étude.

Because of the warming caused by climate change, most Europe experiences a decrease of favourable thermal condition days (TCDs) occurrence. It is significant in Central Europe but no significant in Southern Europe as the low near surface temperatures needed for icing precipitation formation are already seldom met (figure 2b). Conversely, Northern and North-Eastern Europe, which can be affected by temperatures colder than those required for icing precipitation, experience an increase of favourable thermal condition days (TCDs) occurrence. Indeed, regional climate warming lead to more frequent temperatures ranging within the bounds of icing precipitation formation. High-impact icing precipitation is expected to occur when the thermal and vulnerability conditions are simultaneously met. As previously said, day when impactful icing precipitation is expected is referred as "high-impact Icing Precipitation favourable Day" (IPD). Figures 3a and 3b show that IPDs most often occur in mountainous areas and in Northern and North-Eastern Europe. Our results are consistent with Kämäräinen *et al.* (2018). Between 1951-1984 and 1985-2018, even though 48% of Europe area experience a decrease of IPD occurrence reaching in some regions -200 IPDs (e.g. Italian Alps), it is mostly non-significant (figure 3c). Conversely, 47% of Europe area display an increase of IPD occurrence in Northern and Eastern Europe reaching +320 IPDs in the Norwegian Alps.

Figure 3d shows the map of the most influential surface condition explaining the observed IPDs trend. Despite a slightly fragmented pattern, some consistent regions emerge. Regions where thermal condition (TCD) dominates significant negative IPD trends are the UK, Belgium, the Netherlands, Denmark and Germany. The negative IPD trend is associated with an increase in temperature (figures 1b and 1c). As these regions do not necessarily experience frequent much lower temperatures than the temperature thresholds for IPD, regional climate warming makes thermal conditions less frequent (figure 2b). In Southern Europe, observed significant negative IPD trends are also mainly influenced by the thermal condition day (TCD) evolution (figure 3d), because of the increase in temperature (figures 1b and 1c) which reduce the occurrence of TCD that are already seldom met, except in mountainous locations (non-significant trend; figure 2b). Northern and North-Eastern Europe display significant positive observed IPD trends. The most influential conditions explaining the observed IPD trend are more uncertain. It is mostly associated with increasing precipitation (and therefore with VCD) in the Norwegian Alps, in the Baltic countries, Poland, Belarus and Ukraine even though locally the increasing temperature (figures 2b and 2c), leading increase in the TCDs (figure 3d), is the most explanatory influence.

2.2. Euro-CORDEX regional climate simulations

The ERA5 reanalysis is used as a reference data set for bias correction of the Euro-CORDEX simulations. A comparison between the E-OBS data set and the ERA5 reanalysis allows to quantify the uncertainty of the reference data sets often used for regional climate simulation evaluation. With respect to E-OBS, ERA5 reanalysis overestimates the number of days for which the VCD are met in most part of Europe (86% of the domain area; not show), especially over the mountainous regions where overestimation can exceed 2000 days. Such result is consistent with (Rivoire *et al.*, 2021) showing a slight overestimation of wet days in ERA5 reanalysis with respect to E-OBS leading to an excess of mean precipitation in all European regions and particularly over Norwegian Alps (Bandhauer *et al.*, 2022). ERA5 reanalysis also slightly overestimate with respect to E-OBS the number of days for which the TCD are met over 76% of the domain area (not show).

A consequence is that ERA5 overestimates the number of IPDs with respect to E-OBS over 83% of the domain area, especially over mountainous areas where it can reach +400 IPDs between 1972 and 2005 (figure 4a). Therefore, Euro-CORDEX regional climate simulations used in this study generally overestimate the number of IPDs (60% of the studied domains; figure 4b), especially over Norwegian mountains. Conversely, models tend to robustly underestimate the number of IPD in all the alpine massifs. Over the rest of the domain, there is inter-model variability (34% of the grid points for which less than 4 of the 5 models agree about the sign of the difference with E-OBS in terms of IPDs detection).

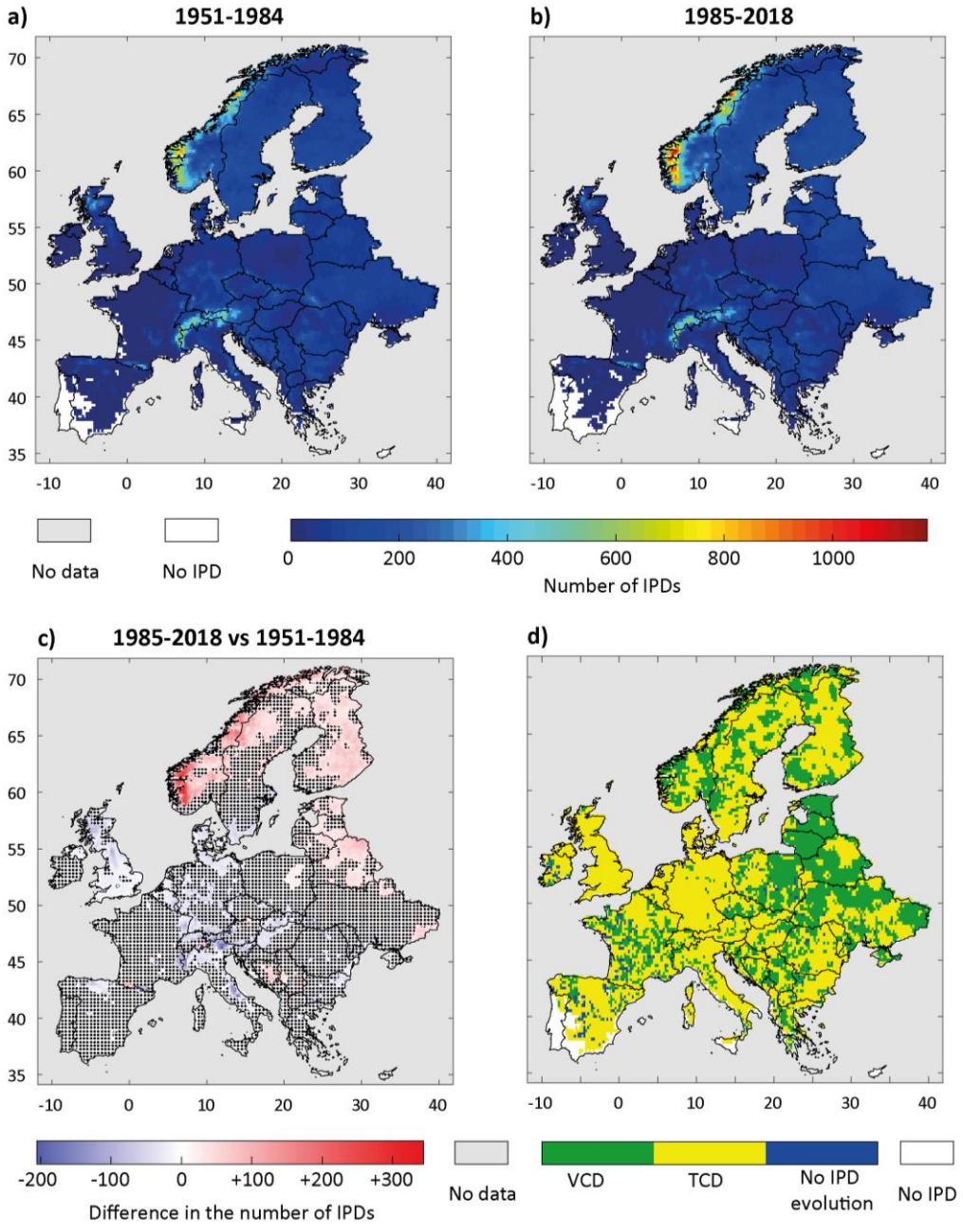

Figure 3. Number of high-impact icing precipitation favourable days (IPDs) over Europe for the periods 1951-1984 (a) and 1985-2018 (b). The number of IPDs is computed through a binary matrix, with "1" when the vulnerability condition day (VCD) and the thermal condition day (TCD) are simultaneously met, and "0" when it is not the case. The difference in the number of IPDs between the both periods is shown on the panel c). No significant differences are indicated with black dotted lines, according to the χ^2 test (at the 0.95 confidence level). The panel d) shows the most influential surface climate variables on IPDs evolution between the both periods (the vulnerability condition day "VCD" in green, or the thermal condition day "TCD" in yellow). In blue, the grid points that show no evolution in the number of IPDs. In grey, sectors with no data in this study. For panel a), b) and d), sectors in white are without IPDs.

Nombre de jours favorables aux précipitations givrantes à fort impact (IPD) sur l'Europe pour les périodes 1951-1984 (a) et 1985-2018 (b). Le nombre d'IPD est calculé à l'aide d'une matrice binaire, avec "1" lorsque le jour de condition de vulnérabilité (VCD) et le jour de condition thermique (TCD) sont simultanément atteints, et "0" lorsque ce n'est pas le cas. La différence dans le nombre d'IPD entre les deux périodes est indiquée sur le panel c). L'absence de différence significative est indiquée par des pointillés noirs, selon le test du χ^2 (au niveau de confiance de 0,95). Le panel d) montre les variables climatiques de surface les plus influentes sur l'évolution des IPD entre les deux périodes (le jour de condition de vulnérabilité "VCD" en vert, ou le jour de condition thermique "TCD" en jaune). En bleu, les points de grille qui ne montrent aucune évolution du nombre d'IPD. En gris, les secteurs pour lesquels il n'y a pas de données dans cette étude. Pour les panels a), b) et d), les secteurs en blanc sont sans IPD.

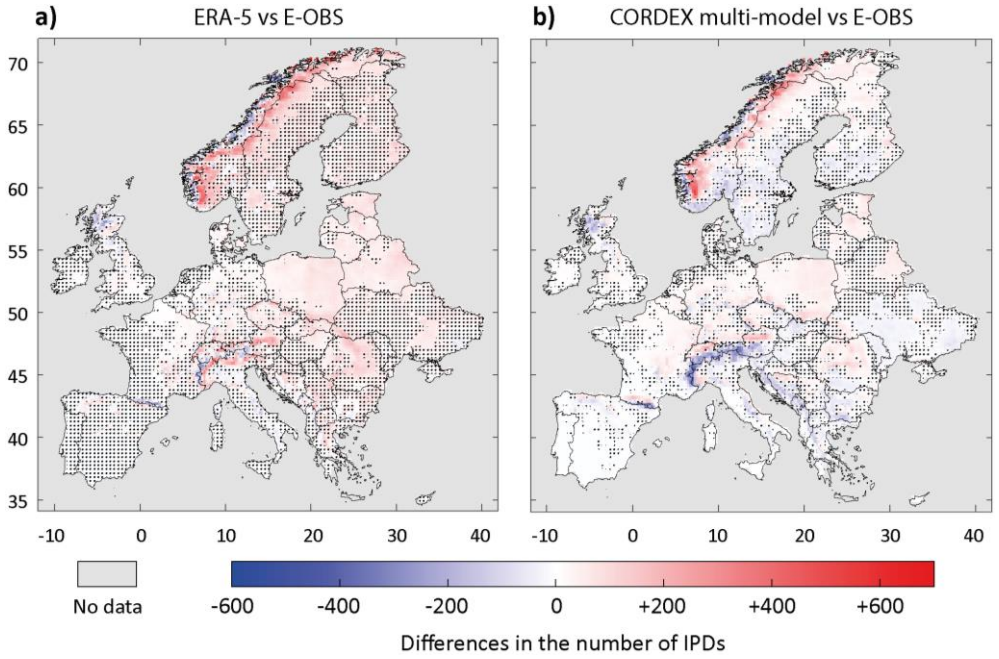

Figure 4. Difference in the number of high-impact icing precipitation favourable days (IPDs) detected in a) the ERA5 reanalysis and b) the Euro-CORDEX multi-model mean (CCLM4, HIRHAM5, RACMO22E, RCA4 and WRF381P), in comparison to the E-OBS reference data series for the 1972-2005 period. The number of IPDs is computed through a binary matrix, with "1" when the vulnerability condition day (VCD) and the thermal condition day (TCD) are simultaneously met, and "0" when it is not the case. For ERA5 reanalysis (panel a), black dotted lines indicated no significant differences according to the χ^2 test (at the 0.95 confidence level). For the multi-model mean (panel b), differences not robust are indicated with black dotted lines, *i.e.* if less than 4 of the 5 models agree about the sign of the difference with E-OBS in terms of IPDs detection. In grey, sectors with no data in this study.

Différence entre le nombre de jours favorables aux précipitations givrantes à fort impact (IPD) détectés dans a) la réanalyse ERA5 et b) la moyenne multi-modèle Euro-CORDEX (CCLM4, HIRHAM5, RACMO22E, RCA4 et WRF381P), par rapport aux données de référence de l'E-OBS, pour la période 1972-2005. Le nombre d'IPD est calculé à l'aide d'une matrice binaire, avec "1" lorsque le jour de condition de vulnérabilité (VCD) et le jour de condition thermique (TCD) sont simultanément atteints, et "0" lorsque ce n'est pas le cas. Pour la réanalyse ERA5 (panel a), les pointillés noirs indiquent qu'il n'y a pas de différences significatives selon le test du χ^2 (au niveau de confiance de 0,95). Pour la moyenne multi-modèle (panel b), les différences non robustes sont indiquées par des pointillés noirs, c'est-à-dire si moins de 4 des 5 modèles sont d'accord sur le signe de la différence avec E-OBS en termes de détection des IPDs. En gris, les secteurs sans données dans cette étude.

3. Future climate projections of IPDs

Figure 5a displays the change of VCDs at short-term time horizon (2026-2059 with respect to 1972-2005) and long-term time horizon (2065-2098 with respect to 1972-2005) for intermediate (RCP4.5) and high (RCP8.5) emission levels. There is a clear North-South divide in Europe. The number of VCDs is expected to increase in Central and Northern Europe (about 80% of the whole studied grid-points showing future increase in VCDs, whatever the horizon or the RCP scenario). A robust increase is simulated for short-term time horizon over 32% and 42% of the relevant area for RCP4.5 and RCP8.5, respectively (figure 5a; left panel) and over 56% and 70% of the relevant area for long-term time horizon (figure 5a; right panel). Conversely, in Southern Europe, a decrease of VCDs is expected for the short-term time horizon in robust way for 9% and 37% of the relevant area for RCP4.5 and RCP8.5, respectively (figure 5a; left panel) and over 38% and 60% of the relevant area for long-term time horizon (figure 5a; right panel). With respect to the observed trend (figure 2), the region of significant increase of VDCs expands over Northern and Central Europe, whereas the region of significant decrease moves Southwards.

Figure 5b displays the change of TCDs at short-term time horizon (2026-2059 with respect to 1972-2005) and long-term time horizon (2065-2098 with respect to 1972-2005) for intermediate (RCP4.5) and high (RCP8.5) emission levels.

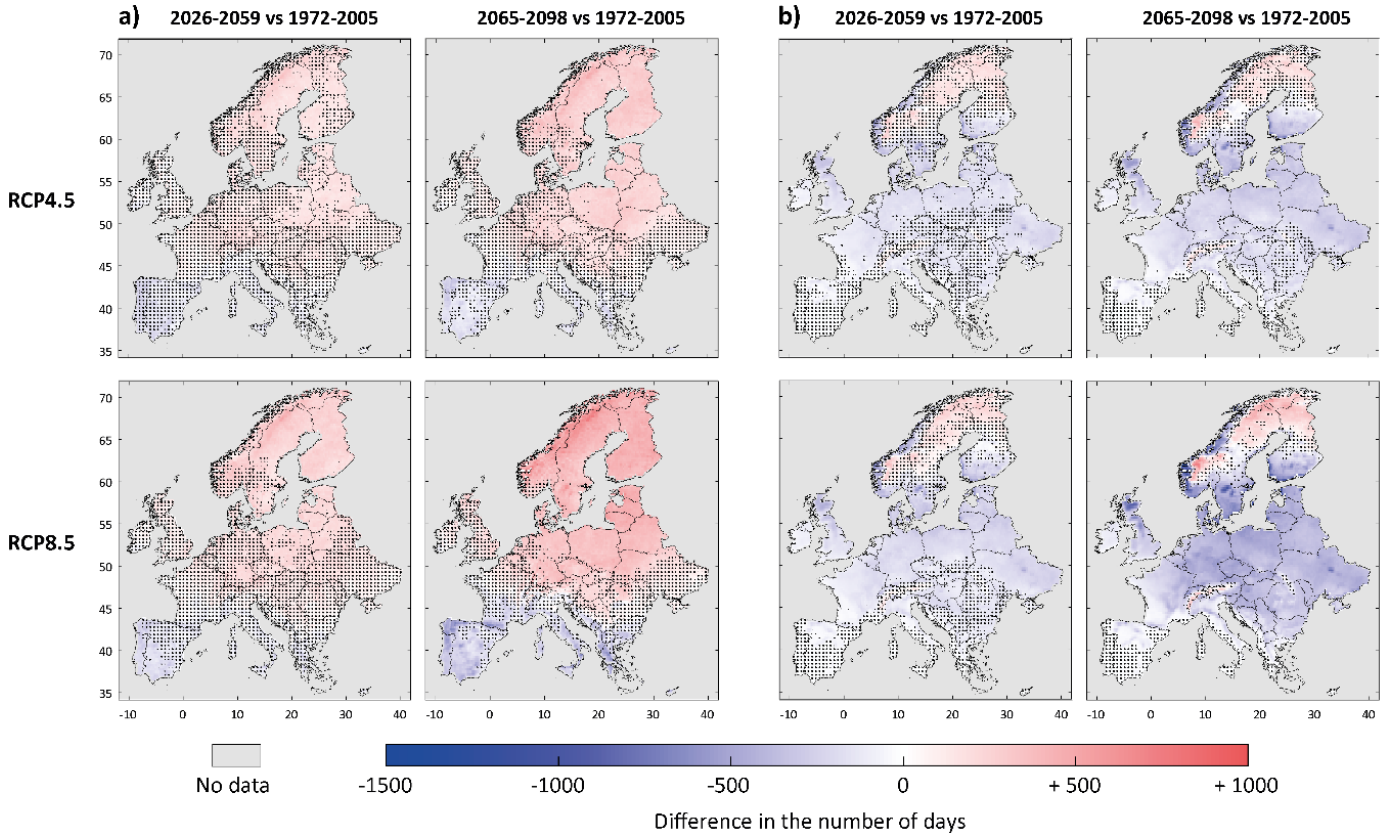

Figure 5. Multi-model means spatiotemporal variability about a) the vulnerability condition day (VCD, precipitation accumulation ≥ 5 mm/day) and b) the thermal condition day (TCD, daily $T^{min} \geq -5°C$ and $T^{max} \leq +2°C$), favourable to the occurrence of high-impact icing precipitation days (IPDs) when they occur simultaneously. For both conditions, the results are show for the near horizon (2026-2059 period, left panel) and the long-term horizon (2065-2098 period, right panel), in comparison to the historical period (1972-2005 period). The upper panel is for the RCP4.5 trajectories (Representative Concentration Pathway) and the lower panel is for the RCP8.5 trajectories. The number of days is computed through a binary matrix, with "1" when the VCD or TCD are met, and "0" when it is not the case. The five models are: CCLM4, HIRHAM5, RACMO22E, RCA4 and WRF381P. Results not robust are indicated with black dotted lines, *i.e.* if less than 4 of the 5 models show statistical significant evolution, according to the χ^2 test (at the 0.95 confidence level).

Variabilité spatio-temporelle des moyennes multi-modèles concernant a) le jour de condition de vulnérabilité (VCD, accumulation de précipitations ≥ 5 mm/jour) et b) le jour de condition thermique (TCD, T^{min} journalière ≥ -5◦C et $T^{max} \leq$ +2◦C), favorable à l'occurrence de jours de précipitations verglaçantes (IPDs) à fort impact lorsqu'ils se produisent simultanément. Pour les deux conditions, les résultats sont présentés pour l'horizon proche (période 2026-2059, panel de gauche) et l'horizon à long terme (période 2065-2098, panel de droite), en comparaison avec la période historique (période 1972-2005). Le panel supérieur correspond au scénario RCP4.5 (Representative Concentration Pathway) et le panel inférieur au scénario RCP8.5. Le nombre de jours est calculé à l'aide d'une matrice binaire, avec "1" lorsque le VCD ou le TCD sont respectés, et "0" lorsque ce n'est pas le cas. Les cinq modèles sont les suivants : CCLM4, HIRHAM5, RACMO22E, RCA4 et WRF381P. Les résultats non robustes sont indiqués par des pointillés noirs, c'est-à-dire si moins de 4 des 5 modèles présentent une évolution statistiquement significative, selon le test du χ^2 (au niveau de confiance de 0,95).

The pattern is very similar to that observed for the recent part between 1951-1984 and 1985-2018 (figure 2) but the significant change expands over a much larger area. A decrease of TCDs is simulated for about 85% of the studied domain, whatever the horizon or the RCP scenario. For short-term time horizon, the decrease of TCDs is in a robust way for 65% and 76% of the relevant area for RCP4.5 and RCP8.5, respectively (figure 5b; left panel) and for 83% and 91% of the relevant area for long-term time horizon (figure 5b; right panel). Conversely, the positive TCDs trend over Scandinavia is in robust way for 35%, 45%, 43% and 80% of the relevant area for RCP4.5 and RCP8.5, respectively, and represent between 12% and 17% of the studied domain.

As for the historical period, with a more straightforward change in the temperatures than the precipitations, Figure 5 confirms that the uncertainty of future climate projections also differ on the projected variables. For both near and long-term time horizons and all RCP scenarios, only from 27% to 67% of the grid points studied show robust future trend for the VCD (relating to the precipitations), compared with 59% to 90% for the TCD (relating to the temperatures). It confirms that the future spatiotemporal evolution of the temperatures over Europe is therefore less uncertain than for the precipitations.

For both near and long-term time horizons and all RCP scenarios, most of Europe should be affected by a decrease of IPDs (between 82% and 93% of the studied domain), except for parts of Scandinavia where an increase of IPDs is projected (figure 6, left panels). These results are consistent with Kämäräinen *et al.* (2018). In our study, only 8% to 18% of the domain area display robust reduction of IPDs for RCP4.5 scenario, and 12% to 48% of the domain area for RCP8.5 scenario. As show in the right panels, the projected trend of IPDs in Europe is mainly explained by the increase of temperatures (TCD; between 90% and 97% of the studied domain). The weakest uncertainty associated with the temperature projections provide good confidence in the future decline in the number of high-impact icing precipitation favourable days over most of Europe.

However, in the Scandinavian Peninsula, the situation is more contrasted than for the rest of Europe. The IPDs trend is negative along the western coast and the Norwegian Alps, whereas it is mainly positive eastwards. The negative trend is associated to an increase of temperatures (TCD; figure 6, right panel). Indeed, most of Norway has a maritime climate with mild winters and cool summers. Because of the influence of the North Atlantic Ocean, Norway has a much warmer climate than its latitudinal position would indicate. Conversely, winter and summer temperature differences in Sweden are extreme, but generally the country enjoys a temperate climate, thanks to the North Atlantic Drift (extension of the Gulf Stream). Above the Arctic Circle, winter is severe with temperatures going below -30°C. That is why part of the IPDs positive trend is attributable to increase of precipitation (VCD), but associated with higher uncertainty than for the IPDs negative trend affecting most of Europe.

4. Discussion

As mentioned in the study, the E-OBS observed reference data covering the historical period (1951-2018) contains inevitably some errors and uncertainties mainly due to the sensitivity of the interpolation to the spatial and temporal coverage of the meteorological stations used to create this dataset, especially for the precipitation series. Others precipitation data sets covering Europe from observations could have been considered for the historical period, such as from the Global Precipitation Climatology Project (GPCP; Huffman *et al.*, 2001) or the National Oceanic and Atmospheric Administration (NOAA) Climate Prediction Center (CPC; Chen *et al.*, 2008). The GPCP database is different from the E-OBS since it merges observations with satellite series, but are only available from January 1979 for the most recent version. The CPC also covers shorter period than E-OBS, from 1979 to 2005.

In this study, the precipitation observations are used with a threshold of 5 mm to consider wet days favourable to the occurrence of an high-impact icing precipitation, which helps to increase confidence in the use of the E-OBS data series because mainly extreme precipitation values tend to be uncertain in this dataset (Haylock *et al.*, 2008; Hofstra *et al.*, 2010). Given the spatio-temporal coverage of the E-OBS dataset, and the number of previous studies that already have relied on it (Kjellström *et al.*, 2010; Flaounas *et al.*, 2012; Stefanon *et al.*, 2012; Kjellström *et al.*, 2013; Stefanon *et al.*, 2014; Vaittinada *et al.*, 2016; Raymond *et al.*, 2016; Drobinski *et al.*, 2018; Raymond *et al.*, 2018a and 2018b), the E-OBS daily data set is a good compromise to study the daily observed temperature and precipitation fields over Europe from the middle of the 20th century until the present days.

The results obtained in this study for the future period are partly model-dependent (from the Euro-Cordex regional models, and from the CMIP-5 global models that drive the regional ones).

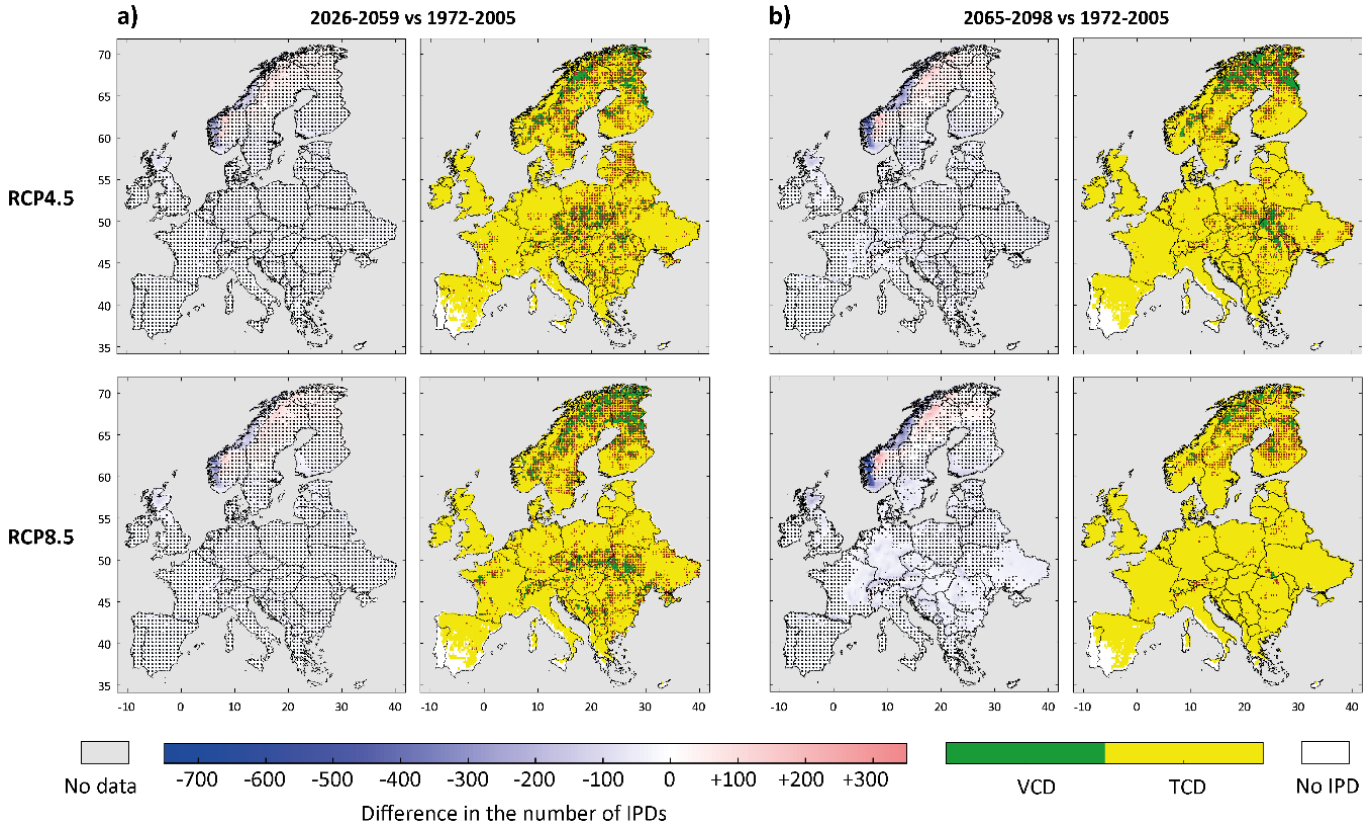

Figure 6. Multi-model means spatiotemporal variability in the number of high-impact icing precipitation favourable day (IPDs, left panels) and the indications of the most influential surface climate variables on IPDs evolution (the vulnerability condition day "VCD" in green, or the thermal condition day "TCD" in yellow, right panels). Evolutions are studied for a) the near horizon (2026-2059 period) and b) the long-term horizon (2065-2098 period), in comparison to the historical period (1972-2005 period). The upper panel is for the RCP4.5 trajectories (Representative Concentration Pathway) and the lower panel is for the RCP8.5 trajectories. The number of IPDs is computed through a binary matrix, with "1" when VCD and TCD are simultaneously met, and "0" when it is not the case. The five models are: CCLM4, HIRHAM5, RACMO22E, RCA4 and WRF381P. For the left panels, results not robust are indicated with black dotted lines, *i.e.* if less than 4 of the 5 models show statistical significant result in terms of evolution in the number of IPDs, according to the χ^2 test (at the 0.95 confidence level). For the right panels, red dotted lines indicate that less than 4 of the 5 models are agree about the most influential climate variable (precipitations 'VCD" or temperatures "TCD") related to the IPDs evolution.

Variabilité spatio-temporelle multi-modèles du nombre de jours favorables aux précipitations givrantes à fort impact (IPDs, panel de gauche) et indications des variables climatiques de surface les plus influentes sur l'évolution des IPDs (le jour de condition de vulnérabilité "VCD" en vert, ou le jour de condition thermique "TCD" en jaune, panel de droite). Les évolutions sont étudiées pour a) l'horizon proche (période 2026-2059) et b) l'horizon à long terme (période 2065-2098), en comparaison avec la période historique (période 1972-2005). Le panel supérieur correspond au scénario RCP4.5 (Representative Concentration Pathway) et le panneau inférieur au scénario RCP8.5. Le nombre d'IPD est calculé à l'aide d'une matrice binaire, avec "1" lorsque la VCD et la TCD sont simultanément respectées, et "0" lorsque ce n'est pas le cas. Les cinq modèles sont les suivants : CCLM4, HIRHAM5, RACMO22E, RCA4 et WRF381P. Pour les panels de gauche, les résultats non robustes sont indiqués par des pointillés noirs, c'est-à-dire si moins de 4 des 5 modèles présentent un résultat statistiquement significatif en termes d'évolution du nombre d'IPD, selon le test du χ^2 (au niveau de confiance de 0,95). Pour les panels de droite, les pointillés rouges indiquent que moins de 4 des 5 modèles sont d'accord sur la variable climatique la plus influente (précipitations "VCD" ou températures "TCD") liée à l'évolution des IPDs.

As mentioned by Hawkins and Sutton (2009), uncertainties in the simulations are due to the model formulation (model uncertainties), to the scenario uncertainties, and from the random internal variability of the climate system. The scenario uncertainties (the choice of RCP 4.5 and RCP 8.5 scenarios) are due to the unknown evolution of the anthropogenic forcings. As explained by Hawkins and Sutton (2011), the model uncertainties are due to the fact that each model projects slightly different

future evolution in response to the same radiative forcings, because of their respective formulations. Von Trentini *et al.* (2019) confirm that the internal variability of the climate system adds significant uncertainties to the projections of the climate evolution, especially for the precipitation parameter. Consequently to these three sources of uncertainties in the climate simulations, there are slight differences between the five models in terms of IPDs, because all our result are not robust (all the five models not always agreed). However, strong robust signals are highlighted in our study, in particular on the future evolution of the vulnerability (VCD) and the thermal (TCD) conditions.

As previously said, our study is a follow-up from the work by Kämäräinen *et al.* (2018), which quantified the trend of freezing rain in Europe in different emission scenarios, from an estimation based on the thermal profile analysis. Based on the CORDEX simulations performed over Europe, they find that under the RCP8.5 scenario, the frequencies of freezing rain decrease in western, central, and south-eastern Europe by 20–55% and increase in the northern and north-eastern parts of the continent by 0–50% toward the end of the century. In our study, the variability of IPDs occurrence is very consistent with the results of Groisman *et al.* (2016) for the historical period (slight increase in the frequency of freezing rain in Norway), and with the results of Kämäräinen *et al.* (2018) for the future period (global future decrease in the frequency of freezing rain over Europe, except for the northern and north-eastern parts of the continent).

Our study extends the analysis of Kämäräinen *et al.* (2018) by merging freezing rain and wet snow, referred in our study as icing precipitation (IPDs). This choice was motivated by the similar impacts such precipitating events produce. The estimation of icing precipitation is also different from Kämäräinen *et al.* (2018) as it follows the methodology used with measurement from surface weather stations, with a condition on the minimum and maximum temperatures (thermal condition; TCD) and a condition on precipitation accumulation (vulnerability condition; VCD). The approach used in our study meet some needs of the stakeholders, with analysis based on easily accessible surface climate data and rely on risk diagnostics which are used by energy infrastructure managers, or forest planning managers. In this approach, the threshold may vary depending on the vulnerability of the "infrastructures" (energy, forest, etc.). In addition, our study also tries to explore the dominating climate variable controlling the future trends of the IPDs between the temperature (TCD) and the precipitation (VCD), because of the different levels of uncertainty associated to these two variables in the future climatic projections.

About the IPDs variability, another interesting approach could be to explore the atmospheric conditions associated with one or two remarkable events of icing precipitation (such as the one in Slovenia in February 2014 and the one in Italy in January 2017), and try to detect the occurrence of similar atmospheric conditions over Europe for the historical and then for the future climate. Similar methods (analogue methods) are already used to predict precipitation events in the Swiss Alps (Horton *et al.*, 2018) or to explore the conditions associated to the 2018 heatwave in the Iberian Peninsula (Barriopedro *et al.*, 2019). This might help to confirm the variability and trends detected in this study, with a second approach using atmospheric variables well simulated by the global or regional climate model in the following version of the regional simulations (forced by the new CMIP6 initiative).

Conclusion

Icing precipitation (here grouping freezing rain and wet snow) could be climatic events that can result in severe damages (including loss of electrical power, transportation disruptions, economic loss for many sectors and sometime in loss of life). In comparison to the North America, Europe has received much less attention in the literature about these kind of climatic events (mainly focus on one specific event, its causes and consequences) while icing precipitation events have regularly impacted European countries. Then, the objectives of this study were (*i*) to apprehend the actual and future spatio-temporal variability of the impactful icing precipitation events across the whole Europe, and (*ii*) to explore the dominating climate variable controlling the trends of these climatic events between the temperature (thermal conditions; TCD)

and the precipitation (vulnerability conditions; VCD). As shown in our results, for both near and long-term time horizons, most of Europe should be affected by a decrease of IPDs (between 82% and 93% of the studied domain), except for parts of Scandinavia.

However, the motivation of this study was to attribute the observed and projected trend to the evolution of thermal (TCD) and vulnerability (VCD) conditions. Indeed, precipitation projections generally display higher uncertainty than temperature projections in regional climate simulations. At each step of our analysis, the robustness of the results is inferred from the multi-model ensemble. Generally, the temperature changes are indeed significant over a larger area than the accumulated precipitation changes.

There is a clear contribution of the temperature (TCD) as the most influential surface climatic conditions in the future variability of the IPDs. The significant temperature increase, as shown in Figure 1, is probably the main reason why icing precipitation occurrence will decrease in most of Europe. As shown, the projected trend of IPDs in Europe (future decrease in the number of IPDs) is mainly influenced by the evolution of the temperature (future decrease in the numbers of TCDs), for between 90% and 97% of the studied domain, because of the warming observed in the historical period and projected for the future period.

In the Scandinavian Peninsula, the observed trend, whether positive or negative, is significant over a much larger area than for the projected trend. In the climate projections, the negative trend of IPDs occurrence is found along the Western coast and the Norwegian Alps, whereas it is positive in eastern Norway and over a narrow band in Sweden. The transition between a maritime climate in Norway and more continental climate in Sweden could explain such zonal gradient. Where the trend is negative, the evolution of temperatures seems to be the main cause, and give us confidence in the predictions. Conversely, for areas where the trend is positive, the increase of accumulated precipitation seems to be the most explanatory cause, but associated with greater uncertainty.

Acknowledgements. This work was conducted in the frame of the Energy4Climate Interdisciplinary Center (E4C) of Institut Polytechnique de Paris and Ecole des Ponts ParisTech.

Funding. ENEDIS [contract \#2020COLLR0258]; 3rd Programme d'Investissements d'Avenir [ANR-18-EUR-0006-02].

Conflict of interest. The authors declare no conflict of interest. The funders had no role in the design of the study; in the collection, analyses, or interpretation of data; in the writing of the manuscript, or in the decision to publish the results.

Data availability statement. E-OBS data used in this work are made available by ECA&D: www.ecad.eu/download/ensembles/download.php. ERA5 data used in this work are made available by the ECMWF (www.ecmwf.int/en/forecasts/datasets/reanalysis-datasets/era5). Euro-CORDEX data used in this work are made available by the CORDEX initiative (cordex.org/domains/cordex-region-euro-cordex/).

References

Aloysius, N.R., Sheffield, J., Saiers, J.E., Li, H., Wood, E.F., 2016. Evaluation of historical and future simulations of precipitation and temperature in central Africa from CMIP5 climate models. *J. Geophys. Res.: Atmospheres*, 121, 130-152.

Andrei, S., Antonescu, B., Boldeanu, M., Marmureanu, L., Marin, C.A., Vasilescu, J., Ene, D., 2019. An exceptional case of freezing rain in Bucharest (Romania). *Atmosphere*, 10, 673.

Bandhauer, M., Isotta, F., Lakatos, M., Lussana, C., Båserud, L., Izsák, B., Szentes, O., Tveito, O.E., Frei. C., 2022. Evaluation of daily precipitation analyses in E-OBS (v19.0e) and ERA5 by comparison to regional high-resolution datasets in European regions. *Int. J. Climatol.*, 42, 727-747.

Barriopedro, D., Sousa, P.M., Trigo, R.M., Gacia-Herrera, R., Ramos, A.M., 2019. The exceptional Iberian heatwave of summer 2018. *Bull. Am. Meteorol. Soc.*, 101, s15-s19.

Bastin, S., Drobinski, P., Chiriaco, M., Bock, O., Roehrig, R., Gallardo, C., Conte, D., Dominguez Alonso, M., Li, L., Lionello, P., Parracho, A.C., 2019. Impact of humidity biases on light precipitation occurrence: observations versus simulations. *Atmos. Chem. Phys.*, 19, 1471-1490.

Bendel, W.B. and Paton, D., 1981. A review of the effect of ice stomrs on thepower industry. *JAMC*, 20, 1445-1449.

Bernstein, B.C., 2000. Regional and local influences on freezing drizzle, freezing rain, and ice pellet events. *Weather and Forecasting*, 15, 485-508.

Bonelli, P., Lacavall, M., Marcacci, A.P., Mariani, G., Stella, G., 2011. Wet snow hazard for power lines: a forecast and alert system applied in Italy. *Nat. Hazards Earth Syst. Sci.*, 11, 2419-2431.

Bourguin, P., 2000. A method to determine precipitation types. *WAF*, 15, 583-592.

Broström, E., 2007. *Ice storm modelling in transmission system reliability calculations*. Thesis of the School of Eletrical Engineering Electric Power Systems, Royal Institute of Technology, Stockholm, Sweden, 117pp.

Bulygina, O.N., Arzhanova, N.M., Groismann, P.Y., 2015. Icing conditions over Northern Eurasia in changing climate. *Environ. Res. Let.*, 10, 025003.

Call, D.A., 2010. Changes in ice storm impacts over time: 1886–2000. *Weather, Climate, and Society*, 2, 23-35.

Caloiero, T., Coscarelli, R., Ferrari, E., Sirangelo, B., 2015. Analysis of dry spells in Southern Italy (Calabria). *Water*, 14, 3009-3023.

Carrière, J.M., Lainard, C., Le Bot, C., Robart, F., 2000. A climatological study of surface freezing precipitation in Europe. *Meteor. Appl.*, 7, 229-238.

Carvalho, D., Cardoso Pereira, S., Rocha, A., 2021. Future surface temperatures over Europe according to CMIP6 climate projections: an analysis with original and bias-corrected data. *Clim. Ch.*, 167, 10.

Changnon, S.A., 2003. Characteristics of ice storms in the United States. *JAMC*, 42, 630-639.

Changnon, S.A. and Bigley, R., 2005. Fluctuations in us freezing rain days. *Clim. Change*, 69, 229-244.

Chen, M., Shi W., Xie, P., Silva, V.B.S., Kousky, V.E., Higgins, R.W., Janowiak, J.E., 2008. Assessing objective techniques for gauge-based analyses of global daily precipitation. *J. Geophys. Res. Atmos.*, 113, D04110.

Cheng, C.S., Auld, H., Li, G., Klaassen, J., Li, Q., 2007. Possible impacts of climate change on freezing rain in south-central Canada using downscaled future climate scenarios. *Nat. Hazards Earth Syst. Sci*., 7, 71-87.

Cheng, C.S., Li, G., Auld, H., 2011. Possible impacts of climate change on freezing rain using downscaled future climate scenarios: Updated for Eastern Canada. *Atmosphere-Ocean*, 49, 8-21.

Christensen, O.B., Drews, M., Christensen, J.H., Dethloff, K., Ketelsen, K., Hebestadt, I., Rinke, A., 2007. *Technical Report 06-17: The HIRHAM Regional Climate Model Version 5*. Danish Meteorological Institute, Copenhagen.

Cornes, R.C, van der Schrier, G., van den Besselaar, E.J.M., Jones, P.D., 2018. An ensemble version of the E-OBS temperature and precipitation data sets. *J. Geophys. Res.: Atmospheres*, 123, 9391-9409.

Cortinas, J., 2000. A climatology of freezing rain in the Great Lakes region of North America. *Month. Weath. Rev.*, 128, 3574-3588.

Cortinas, J., Bernstein, B.C., Robbins, C.C., Strapp, J.W., 2004. An analysis of freezing rain, freezing drizzle, and ice pellets across the United States and Canada: 1976–90. *WAF*, 19, 377-390.

Degelia, S.K., Christian, J.I., Basara, J.B., Mitchell, T.J., Gardner, D.J., Jackson, S.E., Ragland, J.C., Mahan, H.R., 2016. An overview of ice storms and their impact in the United States. *Int. J. Climatol*., 36, 2811-2822.

Dore, M.H.I., 2003. Forecasting the conditional probabilities of natural disasters in Canada as a guide for disaster preparedness. *Nat. Haz.*, 28, 249-263.

Dosio, A., 2016. Projections of climate change indices of temperature and precipitation from an ensemble of bias-adjusted high-resolution EURO-CORDEX regional climate models. *J. Geophys. Res. Atmos.*, 121, 5488-5511.

Drobinski, P., Da Silva, N., Panthou, G., Bastin, S., Muller, C., Ahrens, B., Borga, M., Conte, D., Fosser, G., Giorgi, F., Güttler, I., Kotroni, V., Li, L., Morin, E., Onol, B., Quintana-Segui, P., Romera, R., Torma, C.Z., 2018. Scaling precipitation extremes with temperature in the Mediterranean: Past climate assessment and projection in anthropogenic scenarios. *Clim. Dyn.*, 51, 1237-1257.

Flaounas, E., Drobinski, P., Borga, M., Calvet, J.C., Delrieu, G., Morin, E., Tartari, G., Toffolon, R., 2012. Assessment of gridded observations used for climate model validation in the Mediterranean region: the HyMeX and MED-CORDEX framework. *Env. Res. Let.*, 7, 024017.

Forbes, R., Tsonevsky, I., Hewsom, T., Leutbecher, M., 2014. Towards predicting high-impact freezing rain events. *ECMWF letter*, 141, 15-21.

Frick, C. and Wernli, H., 2012. Case study of high-impact wet snowfall in Northwest Germany (25–27 November 2005): Observations, dynamics, and forecast performance. *WAF*, 27, 1217-1234.

Gil-Alana, L.A. and Sauci, L., 2019. Temperatures across Europe: evidence of time trends. *Clim. change*, 157, 355-364.

Giorgi, F., Jones, C., Asrar, G.R., 2009. Addressing climate information needs at the regional level: the CORDEX framework. *WMO Bulletin*, 58, 175-183.

Giorgi, F., 2010. Uncertainties in climate change projections, from the global to the regional scale. *EPJ Web of Conferences*, 9, 115-129.

Groisman, P.Y., Bulygina, O.N., Yin, X., Vose, R.S., Gulev, S.K., Hanssen-Bauer, I., Førland, E., 2016. Recent changes in the frequency of freezing precipitation in North America and Northern Eurasia. *Environ. Res. Let.*, 11, 045007.

Haylock, M.R., Hofstra, N., Klein Tank, A.M.G., Klok, E.J., Jones, P.D., New, M., 2008. A European daily high-resolution gridded data set of surface temperature and precipitation for 1950-2006. *J. Geophys. Res.*, 113, D20119.

Hawkins, E. and Sutton, R., 2009. The potential to narrow uncertainty in regional climate predictions. *Bull. Am. Meteorol. Soc.*, 90, 1095-1107.

Hawkins, E. and Sutton, R., 2011. The potential to narrow uncertainty in projections of regional precipitation change. *Clim. Dyn.*, 37, 407-418.

Herrera, S., Gutiérrez, J.M., Ancell, R., Pons, M.R., Frías, M.D., Fernandez, J., 2012. Development and analysis of a 50-year highresolution daily gridded precipitation dataset over Spain (Spain02). *Int. J. Climatol.*, 32, 74-85.

Hersbach, H., Bell, B., Berrisford, P., Hirahara, S., Horanyi, A., Munoz-Sabater, J., Nicolas, J., Peubey, C., Radu, R., Schepers, D., Simmons, A., Soci, C., Abdalla, S., Abellan, X., Balsamo, G., Bechtold, P., Biavati, G., Bidlot, J., Bonavita, M., De Chiara, G., Dahlgren, P., Dee, D., Diamantakis, M., Dragani, R., Flemming, J., Forbes, R., Fuentes, M., Geer, A., Haimberger, L., Healy, S., Hogan, R.J., Holm, E., Janiskova, M., Keeley, S., Laloyaux, P., Lopez, P., Lupu, C., Radnoti, G., de Rosnay, P., Rozum, I., Vamborg, F., Villaume, S., Thépaut, J.N., 2020. The ERA5 global reanalysis. *Q. J. R. Meteorol. Soc.*, 146, 1999-2049.

Hoerling, M., Eischeid, J., Perlwitz, J., Quan, X., Zhang, T., Pegion, P., 2012. On the increased frequency of Mediterranean drought. *J. Clim.*, 25, 2146-2161.

Hofstra, N., Haylock, M., New, M., Jones, P., 2009. Testing E-OBS European high-resolution gridded data set of daily precipitation and surface temperature. *J. Geophys. Res.*, 114, D21101.

Hofstra, N., New, M., McSweeney, C., 2010. The influence of interpolation and station network density on the distributions and trends of climate variables in gridded daily data. *Clim. Dyn.*, 35, 841-858.

Horton, P., Jaboyedoff, M., Obled, C., 2018. Using genetic algorithms to optimize the analogue method for precipitation prediction in the Swiss Alps. *J. Hydrom.*, 556, 1220-1231.

Hu, G., Franzke, C.L.E., 2020. Evaluation of daily precipitation extremes in reanalysis and gridded observation-based data sets over Germany. *Geophys. Res. Let.*, 47, e2020GL089624.

Huffman, G.J., Adler R.F., Morrissey, M.M., Bolvin, D.T., Curtis, S., Joyce, R., McGavock, B., Susskind, J., 2001. Global precipitation at one-degree daily resolution from multisatellite observations. *J. Hydrom.*, 2, 36-50.

IPCC: Summary for Policymakers, 2021. In: Climate Change 2021: The Physical Science Basis. Contribution of Working Group I to the Sixth Assessment Report of the Intergovernmental Panel on Climate Change [Masson-Delmotte, V., Zhai, P., Pirani, A., Connors, S.L., Péan, C., Berger, S., Caud, N., Chen, Y., Goldfarb, L., Gomis, M.I., Huang, M., Leitzell, K., Lonnoy, E., Matthews, J.B.R., Maycock, T.K., Waterfield, T., Yelekçi, O., Yu, R., Zhou, B. (eds.)]. Cambridge University Press.

Jacob, D., Petersen, J., Eggert, B., Alias, A., Christensen, O., Bouwer, L., Braun, A., Colette, A., Déqué, M., Georgievski, G., Georgopoulou, E., Gobiet, A., Menut, L., Nikulin, G., Haensler, A., Hempelmann, N., Jones, C., Keuler, K., Kovats, S., Kröner, N., Kotlarski, S., Kriegsmann, A., Martin, E., van Meijgaard, E., Moseley, C., Pfeifer, S., Preuschmann, S., Radermacher, C., Radtke, K., Rechid, D., Rounsevell, M., Samuelsson, P., Somot, S., Soussana, J.F., Teichmann, C., Valentini, R., Vautard, R., Weber, B., Yiou, P., 2014. EUROCORDEX: New high-resolution climate change projections for European impact research. *Reg. Environ. Chang.*, 14, 563-578.

Kämäräinen, M., Hyvärinen, O., Jylhä, k., Vajda, A., Neiglick, S., Nuottokari, J., Gregow, H., 2017. A method to estimate freezing rain climatology from ERA-Interim reanalysis over Europe. *Nat. Hazards Earth Syst. Sci.*, 17, 243-259.

Kämäräinen, M., Hyvärinen, O., Vajda, A., Nikulin, G., van Meijgaard, E., Teichmann, C., Jacob, D., Gregow, H., Jylhä, K., 2018. Estimates of present-day and future climatologies of freezing rain in Europe based on CORDEX Regional Climate Models. *J. Geophys. Res.: Atmospheres*, 123, 13291-13304.

Kjellström, E., Boberg, F., Castro, M., Christensen, J.H., Nikulin, G., Sánchez, E., 2010. Daily and monthly temperature and precipitation statistics as performance indicators for regional climate models. *Clim. Res.*, 44, 135-150.

Kjellström, E., Thejll, P., Rummukainen, M., Christensen, J.H., Boberg, F., Christensen, O.B., Fox Maule, C., 2013. Emerging regional climate change signals for Europe under varying large-scale circulation conditions. *Clim. Res.*, 56, 103-119.

Klok, E.J. and Klein Tank, A.M.G., 2009. Updated and extended European dataset of daily climate observations. *Int. J. Climatol.*, 29, 1182-1191.

Kumar, S., Merwade, V., Kinter III, J.M., Niyogi, D., 2013. Evaluation of temperature and precipitation trends and long-term persistence in CMIP5 twentieth-century climate simulations. *J. Cli.*, 26, 4168-4185.

Kyselý, J. and Plavcová, E., 2010. A critical remark on the applicability of E-OBS European gridded temperature data set for validating control climate simulations. *J. Geophys. Res.*, 115, D23118.

Lambert, S.J., Hansen, B.K., 2011. Simulated changes in the freezing rain climatology of North America under global warming using a coupled climate model. *Atmosphere-Ocean*, 49, 289-295.

Lemos, G., Semedo, A., Dobrynin, M., Menendez, M., Miranda, P.M.A., 2020. Bias-corrected CMIP5-derived single-forcing future wind wave climate projections toward the end of the twenty-first century. *J. of App. Met. and Clim.*, 59, 1393-1414.

Llasat, M.C., Turco, M., Quintana-Segui, P., Llasat-Botija, M., 2014. The snow storm of 8 March 2010 in Catalonia (Spain): a paradigmatic wet-snow event with a high societal impact. *Nat. Hazards Earth Syst. Sci.*, 14, 427-441.

Makkonen, L. and Wichura, B., 2010. Simulating wet snow loads on power line cables by a simple model. *Cold Reg. Sci. Technol.*, 61, 73-81.

Marcacci, P., Lacavella, M., Pirovano, G., 2019. *Monitoring, measurements and mitigation for wet snow accretion on overhead conductors*. Proceedings – Int. Workshop on

Atmospheric Icing of Structures, 23-28 June 2019, Reykjavik, Finland, 6p.

Markosek, J., 2015. *Severe freezing rain in Slovenia*. Report from the Slovenian Environmental Agency, in Newsletter 20 of the European Forecaster.

Mehran, A., Aghakouchak, A., Philipps, T.J., 2014. Evaluation of CMIP5 continental precipitation simulations relative to satellite-base gauge-adjusted observations. *J. Geophys. Res.: Atmospheres*, 119, 1695-1707.

Michelangeli, P.-A., Vrac, M., Loukos, H., 2009. Probabilistic downscaling approaches: Application to wind cumulative distribution functions. *Geoph. Res. Let.*, 36, L11708.

Moss, R.H., Edmonds, J.A., Hibbard, K.A., Manning, M.R., Rose, S.K., van Vuuren, D.P., Carter, T.R., Emori, S., Kainuma, M., Kram, T., Meehl, G.A., Mitchell, J.F.B., Nakicenovic, N., Riahi, K., Smith, S.J., Stouffer, R.J., Thomson, A.M., Weyant, J.P., Wilbanks, T., 2010. The next generation of scenarios for climate change research and assessment. *Nature*, 463, 747-756.

Noël, T., Loukos, H., Defrance, D., Vrac, M., Levavasseur, G., 2021. A high-resolution downscaled CMIP5 projections dataset of essential surface climate variables over the globe coherent with the ERA5 reanalysis for climate change impact assessments. *Data in Brief*, 35, 106900.

Prein, A.F. and Gobeit, A., 2017. Impacts of uncertainties in European gridded precipitation observations on regional climate analysis. *Int. J. Climatol.*, 37, 305-327.

Rauber, R.M., Ramamurthy, M.K., Tokay, A., 1994. Synoptic and mesoscale structures of a severe freezing rain event: the St. Valentine's day ice storm. *WAF*, 9, 183-208.

Raymond, F., Ullmann, A., Camberlin, P., Drobinski, P., Chateau Smith, C., 2016. Extreme dry spell detection and climatology over the Mediterranean Basin during the wet season. *Geophys. Res. Lett.*, 43, 7196-7204.

Raymond, F., Ullmann, A., Camberlin, P., Oueslati, B., Drobinski, P., 2018a. Atmospheric conditions and weather regimes associated with extreme winter dry spells over the Mediterranean basin. *Clim. Dyn.*, 50, 4437-4453.

Raymond, F., Drobinski, P. Ullmann, A., Camberlin, P., 2018b. Extreme dry spells over the Mediterranean Basin during the wet season: assessment of hymex/med-CORDEX regional climate simulations (1979-2009). *Int. J. Climatol.*, 38, 3090-3105.

Rivoire, P., Martius, o., Naveua, P., 2021. A comparison of moderate and extreme ERA-5 daily 2 precipitations with two observational data sets. *Earth and Space Science*, 8, e2020EA001633.

Rockel, B., Will, A., Hense, A., 2008. The regional climate model COSMO-CLM (CCLM). *Meteorol. Z.*, 17, 347-348.

Rummukainen, M., Räisänen, J., Bringfelt, B., Ullerstig, A., Omstedt, A., Willen, U., Hansson, U., Jones, C., 2001. A regional climate model for northern Europe: model description and results from the downscaling of two GCM control simulations. *Clim. Dyn.*, 17, 339-359.

Sillmann, J., Kharin, V.V., Zhang, X., Zwiers, F.W., Bronaugh, D., 2013. Climate extremes indices in the CMIP5 multimodel ensemble: Part 1. Model evaluation in the present climate. *J. Geophys. Res.: Atmospheres*, 118, 1716-1733.

Skamarock, W., Klemp, J., Dudhia, J., Gill, D., Barker, D., Duda, M., Huang, X., Wang, W., Powers, J., 2008. *A description of the advanced research wrf version 3*. NCAR Technical Note NCAR/TN- 475+STR, NCAR, Boulder.

Solangi, A.R., 2018. *Icing effects on power lines and anti-icing and de-icing methods*. Thesis of the Artic University of Norway, Department of Safety and Engineering, Tromsø, Norway, 89pp.

Stefanon, M., D'Andrea, F., Drobinski, P., 2012. Heatwave classification over Europe and the Mediterranean region. *Environ. Res. Lett.*, 7, 014023.

Stefanon, M., Drobinski, P., D'Andrea, F., Lebeaupin-Brossie, C., Bastin, S., 2014. Soil moisture-temperature feedbacks at meso-scale during summer heat waves over Western Europe. *Clim. Dyn.*, 42, 1309-1324.

Stewart, R.E., Thériault, J.M., Henson, W., 2015. On the characteristics of and processes producing winter precipitation types near 0°C. *Bull. Am. Met. Soc.*, 96, 623-642.

US NWS, 2020. *WFO winter weather products specification*. NWSI report, 10-513, 51pp.

Vaittinada Ayar, P., Vrac, M., Bastin, S., Carreau, J., Déqué, M., Gallardo, C., 2016. Intercomparison of statistical and dynamical downscaling models under the EUROS- and MED-CORDEX initiative framework: present climate evaluations. *Clim. Dyn.*, 46, 1301-1329.

Vaittinada Ayar, P., Vrac, M., Mailhot A, 2021. Ensemble bias correction of climate simulations: preserving internal variability. *Sci. Rep.*, 11, 3098.

Van den Besselaar, E.,J.,M., Klein Tank, A.M.G., Buishand, T.A., 2012. Trends in European precipitation extremes over 1951–2010. *Int. J. Climatol*, 33, 2682-2689.

Van Meijgaard, E., van Ulft, L.H., van de Berg, W.J., Bosveld, F.C., van den Hurk, B., Lenderink, G., Siebesma, A.P., 2008. *Technical Report 302: The KNMI regional atmospheric climate model RACMO version 2.1*. Royal Netherlands Meteorological Institute, De Bilt.

Van Oldenborgh, G.J., Drijfhout, S., van Ulden, A., Haarsma, R., Sterl, A., Severijns, C., Hazeleger, W., Dijkastra, H., 2009. Western Europe is warming much faster than expected. *Clim. Past.*, 5, 1-12.

Velikou, K., Lazoglou, G., Tolika, K., Anagnostopoulou, C., 2022. Reliability of the ERA5 in replicating mean and extreme temperatures across Europe. *Water*, 14, 543.

von Trentini, F., Leduc, M., Ludwig, R., 2019. Assessing natural variability in RCM signals: comparison of a multi model EURO-CORDEX ensemble with a 50-member single model large ensemble. *Clim. Dyn.*, 53, 1963-1979.

Vrac, M., Drobinski, P., Merlo, A., Herrmann, M., Lavaysse, C., Li, L., Somot, S., 2012. Dynamical and statistical

downscaling of the French Mediterranean climate: uncertainty assessment. *Nat. Hazards Earth Syst. Sci.*, 11, 2769-2784.

Vrac, M. and Friederichs, P., 2015. Multivariate-intervariable, spatial, and temporal-Bias correction. *J. Clim.*, 28, 218-237.

Vrac, M., Noël, T., Vautard, R., 2016. Bias correction of precipitation through Singularity Stochastic Removal: Because occurrences matter. *J. Geophys. Res. Atmos.*, 121, 5237-5258.

Xu, Z., Han, Y., Tam, C.y., yang, Z.L., Fu, C., 2021. Bias-corrected CMIP6 global dataset for dynamical downscaling of the historical and future climate (1979–2100). *Sci. data*, 8, 293.

Citation of article: Raymond F., Drobinski P., Roche N., 2023. Attributing icing precipitations trend (1951-2098) in the context of climate change in Europe. *Climatologie*, 21, 1.